Expansion of Nonlinear System Response using Linear Transformation Matrices from Reduced Component Model Representations

Tim Marinone, Louis Thibault, Peter Avitabile
Structural Dynamics and Acoustic Systems Laboratory
University of Massachusetts Lowell
One University Avenue
Lowell, Massachusetts 01854

ABSTRACT

Finite element models of structural systems have become increasingly complicated as they are used for many types of applications. Because a highly detailed model is not required for every purpose, much work has been presented in generating reduced-order models (ROMs) that accurately reflect the dynamic characteristics of the system. Recent work has shown that these ROMs can be used to compute both the linear and nonlinear dynamic response of the structure at the reduced space without loss of accuracy due to the reduction procedures.

Although computationally beneficial to calculate dynamic response at drastically reduced space, there are significant advantages in expanding the response out to the full-field solution. Much work has been focused on the expansion of linear dynamic solutions for improved visualization. This work builds on previous efforts and demonstrates that the transformation matrix generated from the linear model can be used to accurately expand the nonlinear dynamic response; this is true for component as well as system models. Both analytical and experimental cases are examined to demonstrate the accuracy of this technique.

INTRODUCTION

Finite element models of structural systems are often composed of thousands to millions of degrees of freedom (DOF) and are used for many different applications. Analysts want the model to reflect the physical structure as closely as possible, which often requires both modeling using nonlinear elements as well as using test data to verify the model. Because the analyst is under increasing time constraints, there is also a simultaneous interest in generating an efficient model that can be solved very quickly. In order to combine these requirements, reduced order, test verified components are typically used for much of this work.

Even though these reduced order models (ROMs) satisfy the requirements described above, a main disadvantage of ROMS is that they only provide information at the limited number of degrees of freedom (ADOF), and do not provide the full space solution (NDOF). As a result, the transformation matrix used in creating the ROM can also be used to expand the information from ADOF to NDOF at a very low computation cost. Although most of the work in this area has been on expansion of linear mode shapes, Chipman [1] demonstrated that real time operating data could also be expanded using the same transformation matrix, which allowed a better visualization of the response. Pingle [2] further studied this work and demonstrated that linear displacement results from either a model or test data could also be expanded out and used for further post-processing such as strain.

Although this work has been useful for many applications, a variety of models and physical structures are nonlinear in nature. Due to the complex nature of these nonlinear models, the computation time of these models increases drastically, this makes them unwieldy to use. Recent work by Thibault [3] and Marinone [4] involved the development of efficient techniques by treating the nonlinear elements as piecewise linear, which allows multiple linear models to be used depending on the state of the nonlinearity. Figure 1 is a schematic overview of both techniques; Equivalent Reduced Model Technique (ERMT) uses highly accurate physical space ROMs, while Modal Modification Response Technique (MMRT) uses mode superposition in conjunction with structural dynamic modification (SDM).

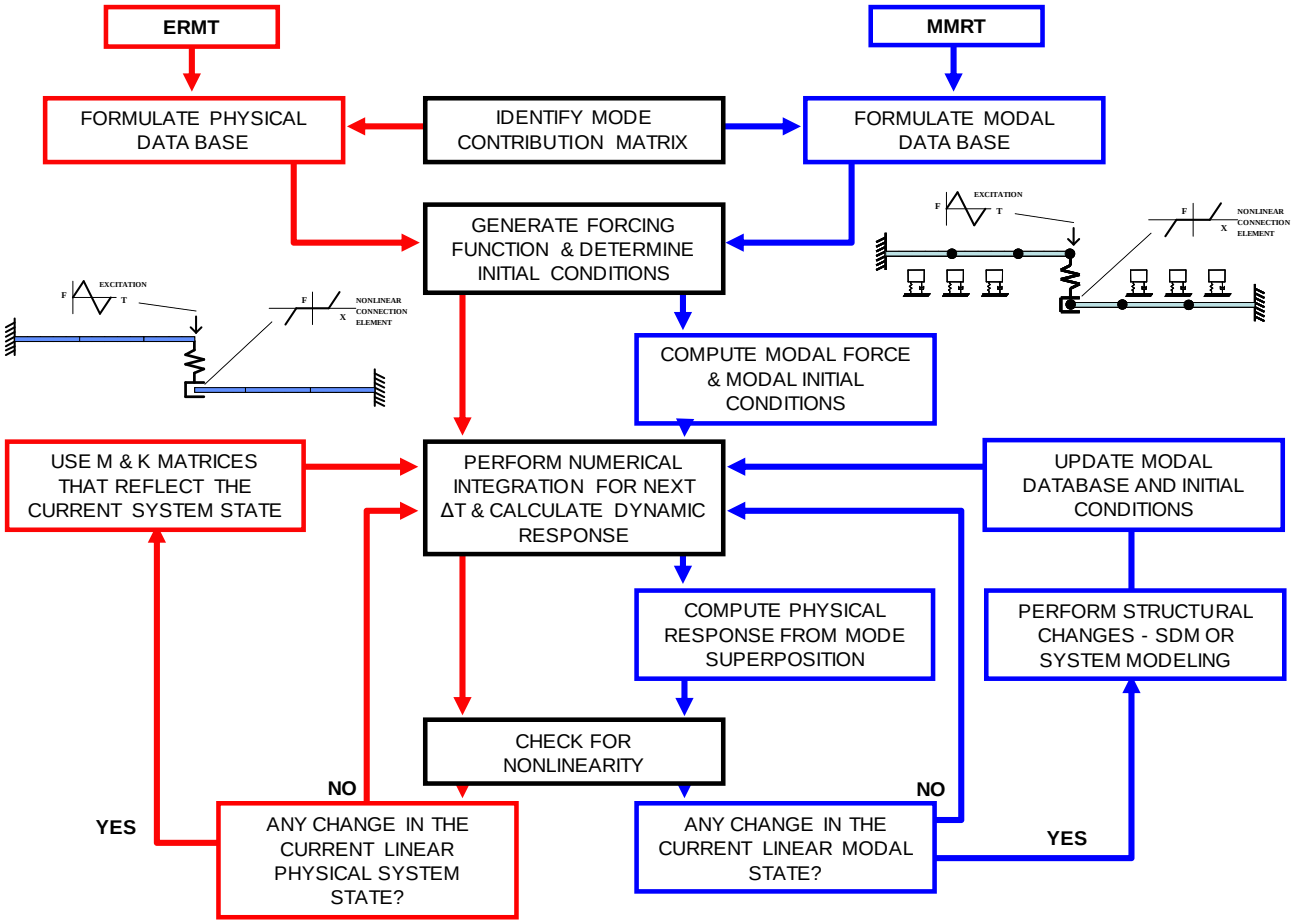

Figure 1. Overview schematic of ERMT and MMRT

While both techniques were shown to be very efficient and accurate, the solution was again solved at the ADOF. Unlike the linear models which only have one transformation matrix, the nonlinear model requires reduced order components for each possible state, which requires multiple transformation matrices to be formed. This paper will show that even though the nonlinear solution may experience multiple system states, only one transformation matrix that spans the modes of interest for all states of the system is needed to expand out the nonlinear response solution from ADOF to NDOF. An overview of model reduction/expansion is provided in the theory, along with system modeling and the mode contribution matrix; this is used to identify the modes that need to be included in the transformation matrices when generating ROMs. Two cases are described in this paper. The first case is an analytical case that shows the results obtained from expanding out the ROM responses are equivalent to the results obtained from solving the full model. The second case is an experimental case showing that experimentally measured data can be expanded out to obtain nonlinear dynamic responses at locations that would be difficult to obtain using traditional transducers, such as rotational DOF or inaccessible locations.

THEORY

The following section presents the theory of model reduction and system modeling needed for the development of the newly proposed methodology.

Model Reduction and Expansion

Model reduction is used to reduce the size of a large analytical model to develop a more efficient model for further analytical studies. The reduced model size also allows for model updating and correlation with test data. Model reduction is performed for a number of reasons, but is used primarily as a mapping technique for the expansion of test data. Active DOF (ADOF) are used to identify the reduced order model; in the experimental case studied, the ADOF correspond to the

tested DOF. Several model reduction methods have commonly been used, which include Guyan Condensation [5], Dynamic Condensation [6], Improved Reduced System (IRS) [7], System Equivalent Reduction Expansion Process (SEREP) [8], and Hybrid-Kammer [9]. While any of these techniques could be used for model reduction, only SEREP is used within this study due to specific advantages that are discussed in the following sections.

General Transformation

To reduce a full set of finite element model (FEM) NDOF to a set of ADOF, a transformation relationship must be determined. This transformation can be written in general terms as

$$\{x_n\} = \begin{Bmatrix} x_a \\ x_d \end{Bmatrix} = [T]\{x_a\} \tag{1}$$

The 'n' subscript denotes the full set of FEM NDOF, the 'a' subscript denotes the active set of DOF (ADOF), and the 'd' subscript denotes the deleted set of DOF (sometimes referred to as omitted DOF); the transformation matrix [T] relates the mapping between these two sets of DOF.

Due to the laws of energy conservation, the transformation matrix can be used to reduce the mass and stiffness matrices, which are related to the full space matrices using the transformation operation given as

$$[M_a] = [T]^T [M_n][T] \tag{2}$$

$$[K_a] = [T]^T [K_n][T] \tag{3}$$

The equation of motion can then be written in reduced 'a' space as

$$[M_a]\{\ddot{x}_a\} + [K_a]\{x_a\} = \{F_a(t)\} \tag{4}$$

The eigensolution is then given by

$$[[K_a] - \lambda[M_a]]\{x_a\} = \{0\} \tag{5}$$

What is most important in model reduction is that the eigenvalues and eigenvectors of the original system are preserved as accurately as possible in the reduction process. If this is not maintained then the matrices are of questionable value. Reduction schemes such as Guyan Condensation [5] and Improved Reduced System (IRS) [7] are based primarily on the stiffness of the system, which results in eigenvalues and eigenvectors that are not exactly reproduced in the reduced order model. However, the System Equivalent Reduction Expansion Process (SEREP) [8] exactly preserves the eigenvalues and eigenvectors in the reduced model.

System Equivalent Reduction Expansion Process (SEREP)

The SEREP [8] transformation matrix $[T_U]$ is developed such that an eigensolution of the resultant reduced mass and stiffness matrices produces the exact frequencies and mode shapes as in the full space model. The SEREP modal transformation relies on the partitioning of the modal equations representing the physical system DOF relative to the modal DOF using

$$\{x_n\} = \begin{Bmatrix} x_a \\ x_d \end{Bmatrix} = \begin{bmatrix} U_a \\ U_d \end{bmatrix}\{p\} = [U_n]\{p\} \tag{6}$$

The relationship for only the ADOF is written as

$$\{x_a\} = [U_a]\{p\} \tag{7}$$

For the case where the number of modes used is less than or equal to the number of ADOF ($a \geq m$), the $[U_a]$ matrix in (7) can be reformulated using a generalized inverse. This results in the least squares solution written as

$$\{p\} = \left([U_a]^T[U_a]\right)^{-1}[U_a]^T\{x_a\} = [U_a]^g\{x_a\} \tag{8}$$

which is then used to relate the full space DOF to the ADOF by substitution back into the modal transformation in (6) and gives

$$\{x_n\} = [U_n][U_a]^g\{x_a\} = [T_U]\{x_a\} \tag{9}$$

Therefore, the SEREP transformation matrix $[T_U]$ is defined as

$$[T_U] = [U_n][U_a]^g \tag{10}$$

The SEREP transformation matrix $[T_U]$ is used either for the reduction of the finite element mass and stiffness matrices, as in (2) and (3), or for the expansion of experimentally measured modal vectors, which is discussed in the following section.

SEREP relies heavily on a "well developed" finite element dynamic model from which an 'n' dimensional eigensolution is obtained for developing the mapping between the full set of FEM NDOF and the reduced set of ADOF. The quality of the results obtained using most reduction processes depends on the selection of ADOF, however this is not a concern when using SEREP. Case studies have been performed to demonstrate the fact that an arbitrary selection of ADOF as well as an arbitrary selection of modes does not affect the mode shapes and frequencies that are preserved in the reduced model when using SEREP [8].

In the situation where the number of modes used is less than the number of ADOF retained in the reduced model ($a > m$), the size of the reduced mass and stiffness matrices are 'a' by 'a', but the rank of the reduced matrices is only 'm'. Therefore, the reduced mass and stiffness matrices are rank deficient and care must be taken when using these reduced matrices. Due to the rank deficiency that results in this scenario, a form of the SEREP reduction process that produces an exact solution can be performed by using the same number of modes as the number of ADOF ($a = m$) for the reduced model.

For the case where the number of ADOF is equivalent to the number of modes retained in the SEREP reduced model, the matrices are fully ranked and well-conditioned. Because the transformation matrix $[T_U]$ is formed from the eigenvectors of the full space finite element model, the reduced matrices preserve the eigenvalues and eigenvectors of the full space model. This implies that any collection of desired eigenvectors can be retained in an exact sense for the reduced model. This fact is significant in terms of the development of efficient models from large finite element models used for forced response studies, especially those that contain discrete nonlinear effects that are typical in joints and connections for many structural systems. The reduced models developed in this work are for the equivalent condition, where the number of modes used is equal to the number of ADOF retained in the reduction process ($a = m$).

An alternate model reduction approach [10] can be used where a highly accurate reduced model is formulated using Guyan Condensation in conjunction with Analytical Model Improvement (AMI). The advantages of this technique are that the desired mode shapes are preserved in an exact sense while the fully ranked and well-conditioned system matrices obtained from the Guyan reduction scheme are also maintained in the process. Further details on this technique are discussed in the paper.

System Modeling and Mode Contribution

Several techniques have commonly been used in structural dynamic studies for generating system models from both analytical and experimental component model representations for a variety of applications. These techniques include physical, modal, frequency based, and hybrid system modeling methods. The proposed approach utilizes system models to represent nonlinear contact and component interconnections as piecewise linear approximations at each time step throughout the forced nonlinear response solution. In this work, a physical to physical system modeling approach is utilized for the cases studied that involve multiple components that can interconnect with one another in a variety of different configurations. Full space physical system models are used to develop a reference solution where the accuracy of the system model is not affected by modal truncation. The mass and stiffness matrices of the full space component models that are used to develop system models are first arranged into a common matrix space, which is shown in Figure 2.

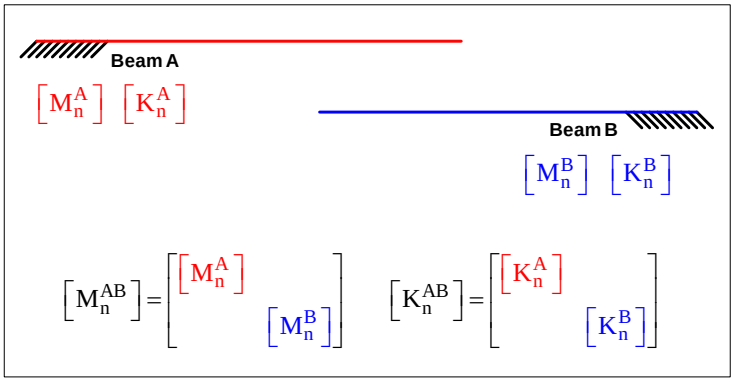

Figure 2. Full Space Component Models Arranged into Common Matrix Space

After the component matrices are arranged into common matrix space, accurate system models are developed for all potential configurations that can occur as the system responds to an input excitation over the frequency range that participates in the system response. The component mass and stiffness matrices can be connected together using coupling or tie matrices, which apply a specified mass or stiffness value that couples a DOF of one component to a DOF of another component. In this work, only stiffness tie matrices are used to demonstrate the proposed methodology; mass effects are also easy to include with this formulation. The equation of motion can then be reformulated in terms of system matrices as

$$\left[\begin{bmatrix} [M_n^A] & \\ & [M_n^B] \end{bmatrix}\right]\left\{\begin{Bmatrix} \ddot{x}_n^A \end{Bmatrix} \\ \begin{Bmatrix} \ddot{x}_n^B \end{Bmatrix}\right\} + \left[\begin{bmatrix} [K_n^A] & \\ & [K_n^B] \end{bmatrix} + [K^{TIE}]\right]\left\{\begin{Bmatrix} x_n^A \end{Bmatrix} \\ \begin{Bmatrix} x_n^B \end{Bmatrix}\right\} = \left\{\begin{Bmatrix} f_n^A \end{Bmatrix} \\ \begin{Bmatrix} f_n^B \end{Bmatrix}\right\} \qquad (11)$$

To illustrate the physical system modeling methodologies employed, the system model formulations that are developed for a two component system with two potential contact locations is discussed below. Figure 3 shows the two component system with two contact locations.

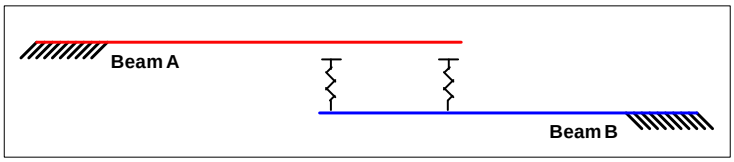

Figure 3. Two Component System with Two Contacts

By further examination of the system in Figure 3, three possible system configurations can be formed during the event that transient response occurs. For configuration 1, only the tip of Beam A is in contact with Beam B. For configuration 2, only the tip of Beam B is in contact with Beam A. For configuration 3, both contacts are engaged. Therefore, three

system models need to be developed using a stiffness tie matrix to connect the components together in each system configuration, which is shown in Figure 4.

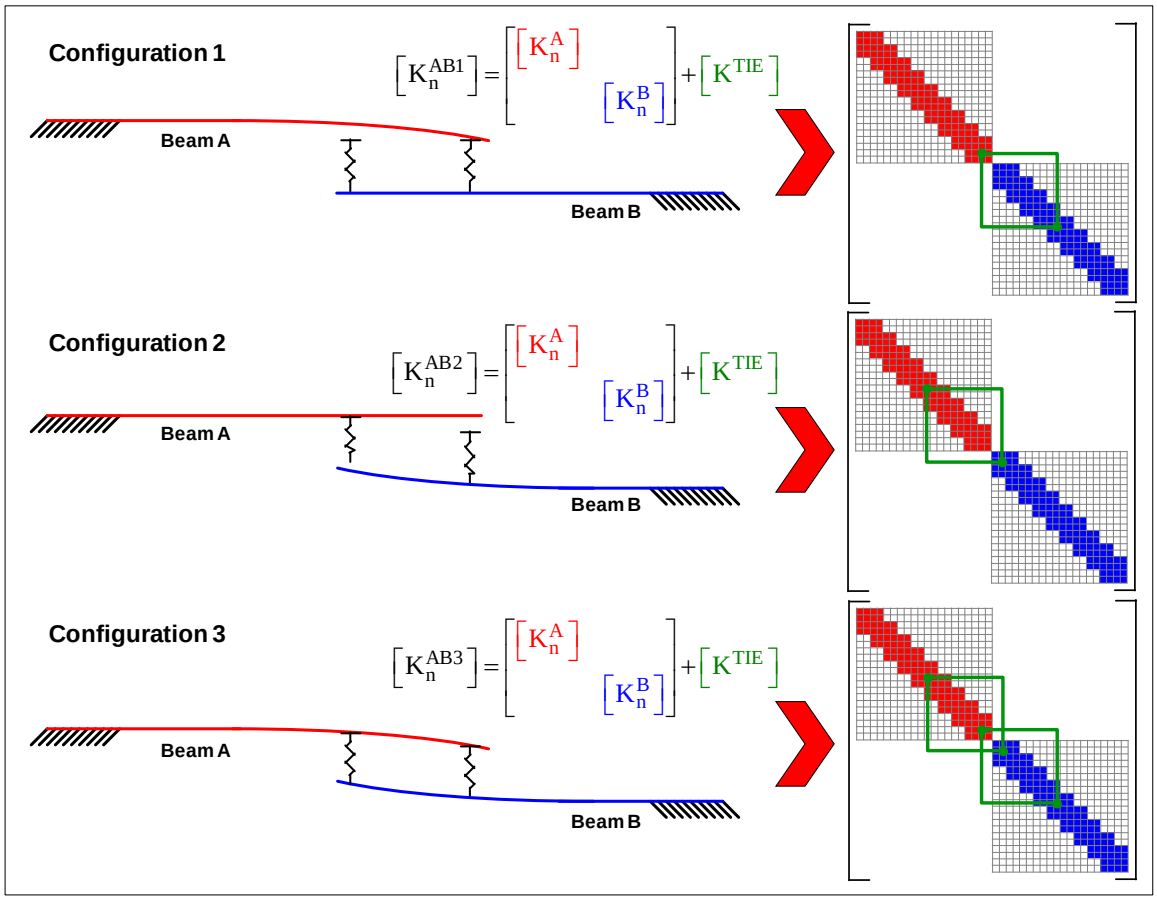

Figure 4. Stiffness Matrix Formulation for Potential System Configurations

Note that small deflection theory is utilized in these analyses where the beams are shown in an exaggerated deformed state for illustrative purposes only. Large geometric displacements are not considered in this analysis for the assembled system configurations shown in Figure 4.

An eigensolution is then computed for each system model using the assembled full space mass and stiffness matrices to obtain the mode shapes and frequencies of each system model. The full space system models are then considered for reduction to a set of ADOF using SEREP. However, to ensure that the reduced models are minimally affected by modal truncation when assembling the system models using multiple reduced component models, the contribution of component modes in the assembled system modes is computed using

$$\text{Mode Contribution} = \begin{bmatrix} [U_n^A] & \\ & [U_n^B] \end{bmatrix}^T [M_n^{AB}][U_n^{AB}] \qquad (12)$$

where $[U_n^A]$ is the matrix of full space FEM mode shapes for component A, $[U_n^B]$ is the matrix of full space FEM mode shapes for component B, $[M_n^{AB}]$ is the full space FEM mass matrix for system AB, and $[U_n^{AB}]$ is the matrix of full space FEM mode shapes for a particular system AB configuration. Note that the system mass matrix $[M_n^{AB}]$ is the same for all system configurations; only the stiffness matrices are modified in the system model assembly process in this work but mass

can easily be added to the set of equations. Details pertaining to the approach used for identifying key contributing modes in the ROMs developed in this work are provided in [3] and [11].

The resulting mode contribution matrix is the key to identifying the necessary set of component modal vectors needed to accurately form the final modified system modes. This is similar to the $[U_{12}]$ matrix that is computed in the Structural Dynamic Modification (SDM) [12] methodology, which is used to identify the modes of the initial unmodified system state that contribute in the modes of the final modified system state. The $[U_{12}]$ matrix or mode contribution matrix contains the scaling coefficients needed to form the final modified set of modes $[U_2]$ from the initial unmodified set of modes $[U_1]$. The $[U_2]$ matrix is written in matrix form as

$$[U_2] = [U_1][U_{12}] \tag{13}$$

Figure 5 illustrates the contribution of the $[U_{12}]$ matrix in forming the final modified system modes $[U_2]$. The 'i^{th}' modified system mode of $[U_2]$ is formed from 'm' modes of the $[U_1]$ matrix multiplied by the first 'm' scaling coefficients of the 'i^{th}' column in the $[U_{12}]$ matrix; these are the red terms shown in Figure 5 and are listed in the following equation.

$$\{u_2\}^{(i)} = \{u_1\}^{(i)} U_{12}{}^{(1i)} + \{u_1\}^{(2)} U_{12}{}^{(2i)} + \cdots \tag{14}$$

While the arrangement of modes are shown sequentially for convenience, only modes that are required in forming the 'm' set of modes need to be included and may not necessarily be sequential. Because all of the 'n' modes are not required in computing the 'i^{th}' system mode of $[U_2]$, the 'n-m' modes shown in blue can be excluded.

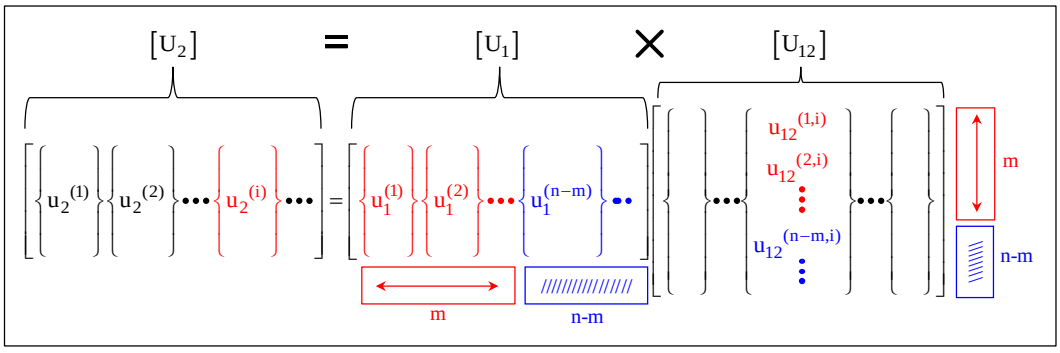

Figure 5. SDM Process Using $[U_{12}]$ Matrix

The mode contribution matrix is then plotted for visual identification of key contributing component modes that are needed to form the system modes. For the two component system with two contact locations, three separate mode contribution matrices need to be computed (one for each system configuration). An example of the mode contribution matrix formulation for system configuration 3 is shown in Figure 6. The various box colors in the mode contribution matrix indicate the amount that each unmodified component mode contributes in a particular modified system mode. Red boxes indicate high levels of contribution, where white boxes indicate minimal or no contribution. The actual contribution ranges for each color are provided in the legend in Figure 6.

To illustrate how the system modes are formed from linear combinations of component modes, the contributing component modes that are needed to form mode 1 for system configuration 3 is shown in Figure 7. The system modes are represented by columns of the mode contribution matrix and the unmodified component modes that are needed to form the system modes are identified along the rows of the mode contribution matrix.

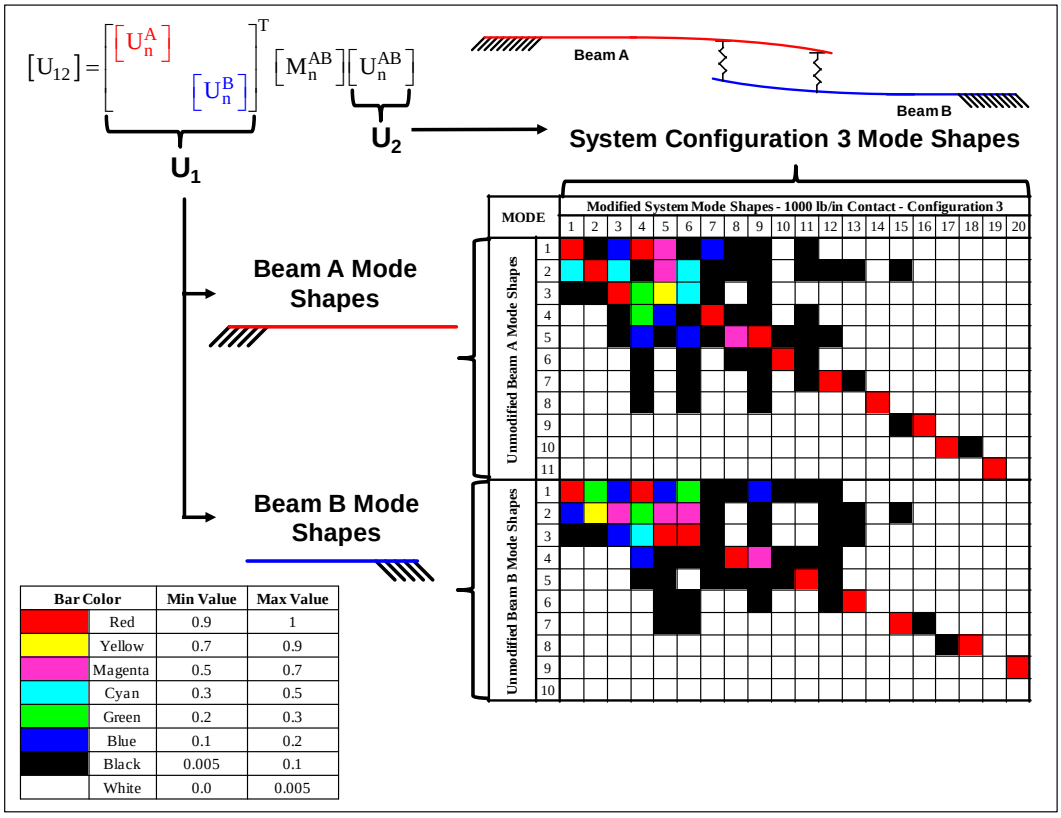

Figure 6. Two Beam System Configuration 3 Mode Contribution Matrix Formulation

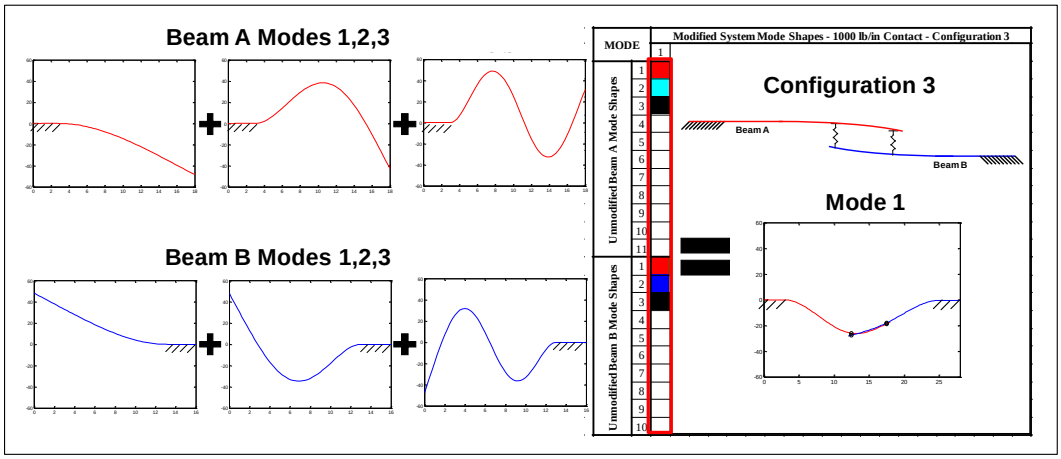

Figure 7. Component Mode Identification for Mode 1 of System Configuration 3

Once the component modes that contribute in each of the system configurations are identified using the mode contribution matrices, the full space system models are reduced to a set of ADOF using SEREP. The model reduction process is shown in Figure 8 for the system configuration 3 model, where the red points indicate the ADOF retained in the reduced order models. The number of ADOF are equal to the number of modes retained in the reduced order models, which preserves the mode shapes and frequencies of the full space component models in an exact sense for the reduced component models. Note that for the a = m case, the quality of the reduced model results obtained using SEREP does not depend on the selection of ADOF and that an arbitrary selection of ADOF as well as an arbitrary selection of modes is permitted.

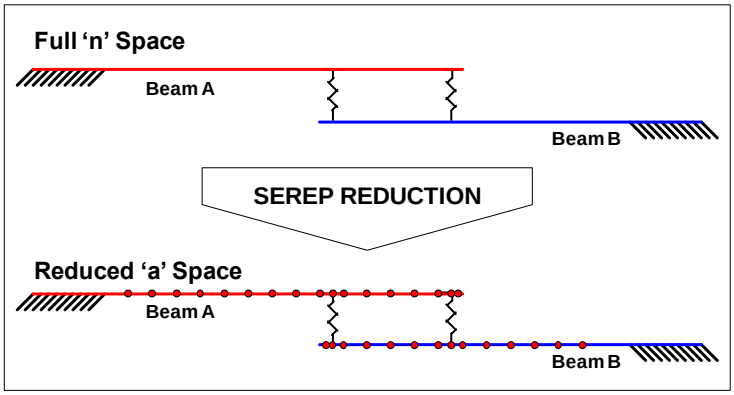

Figure 8. SEREP Reduction of Two Beam System Configuration 3 Model

The reduced system mass and stiffness matrices are then used in the direct integration process for computing the forced nonlinear response, where the equation of motion can be written in reduced space as

$$\left[M_a^{AB}\right]\left\{\ddot{x}_a^{AB}\right\}+\left[K_a^{AB}\right]\left\{x_a^{AB}\right\}=\left\{f_a^{AB}\right\} \tag{15}$$

The $[M_a^{AB}]$ and $[K_a^{AB}]$ matrices reflect the system state at each instance in time of the system response.

Mode Shape and Time Response Data Expansion/Smoothing Process

The expansion of experimentally measured mode shapes is often performed to obtain a full space representation of the mode shape. This is advantageous in cases where the responses at unmeasured translational or rotational DOF are desired, but cannot be measured due to limitations of accessibility, equipment availability, etc. For most of the expansion techniques such as Guyan Condensation [5], Dynamic Condensation [6], and IRS [7], the original data is not modified in the development of the expanded mode shape. The transformation matrix [T] developed using these techniques contains an identity [I] matrix in the ADOF modal vector partition, which implies that the original data is accurate as measured, but this is rarely the case. Therefore, smoothing of the measured data is necessary to remove typical contaminants that exist in any set of measured data. The SEREP expansion process provides the smoothing techniques required to minimize the contaminants that exist in experimentally measured data.

The SEREP transformation matrix $[T_U]$ given in (10) is used to expand and smooth experimentally measured mode shapes from the reduced set of ADOF to the full set of FEM NDOF as

$$[E_n]=[T_U][E_a] \tag{16}$$

where $[E_a]$ is the matrix of experimentally measured mode shapes and $[E_n]$ is the matrix of expanded and smoothed test mode shapes.

This mode shape expansion technique can also be applied to time response data, where the operating deflection shape (ODS) is expanded at each time step from the reduced set of measured ADOF to the full set of FEM NDOF as

$$\{x_n\}=[T_U]\{x_a\} \tag{17}$$

where $\{x_a\}$ is the vector of measured displacements at the reduced set of ADOF for a particular instance in time and $\{x_n\}$ is the vector of expanded and smoothed test displacements for the time instant. This has been performed in previous work by Chipman [1] with real time operating data for improved visualization. This technique was developed further by Pingle [13, 14, 15] to obtain FEA full field response from limited sets of measured data and then further to obtain full field dynamic stress-strain.

Use of Mode Contribution Matrix for Expanding Time Response Data

As described previously, the mode contribution matrix is of critical importance in order to determine the number of modes that are needed to form the final system mode shapes. Because each potential system configuration requires a unique set of modes that can be formed in linear combinations, a unique mode contribution matrix is formed for each configuration. Figure 9 - Figure 11 show the three possible mode contribution matrices for a two beam system with two possible points of contact.

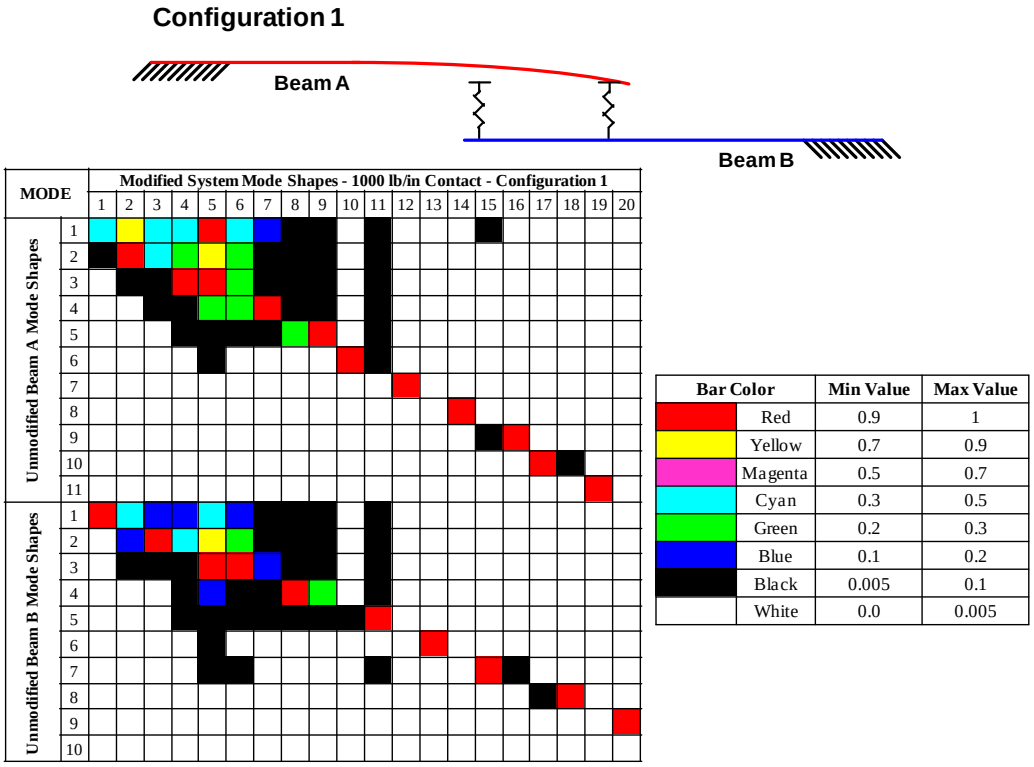

Bar Color	Min Value	Max Value
Red	0.9	1
Yellow	0.7	0.9
Magenta	0.5	0.7
Cyan	0.3	0.5
Green	0.2	0.3
Blue	0.1	0.2
Black	0.005	0.1
White	0.0	0.005

Figure 9. Two Beams with Hard Contacts Config. 1 Mode Contribution Matrix

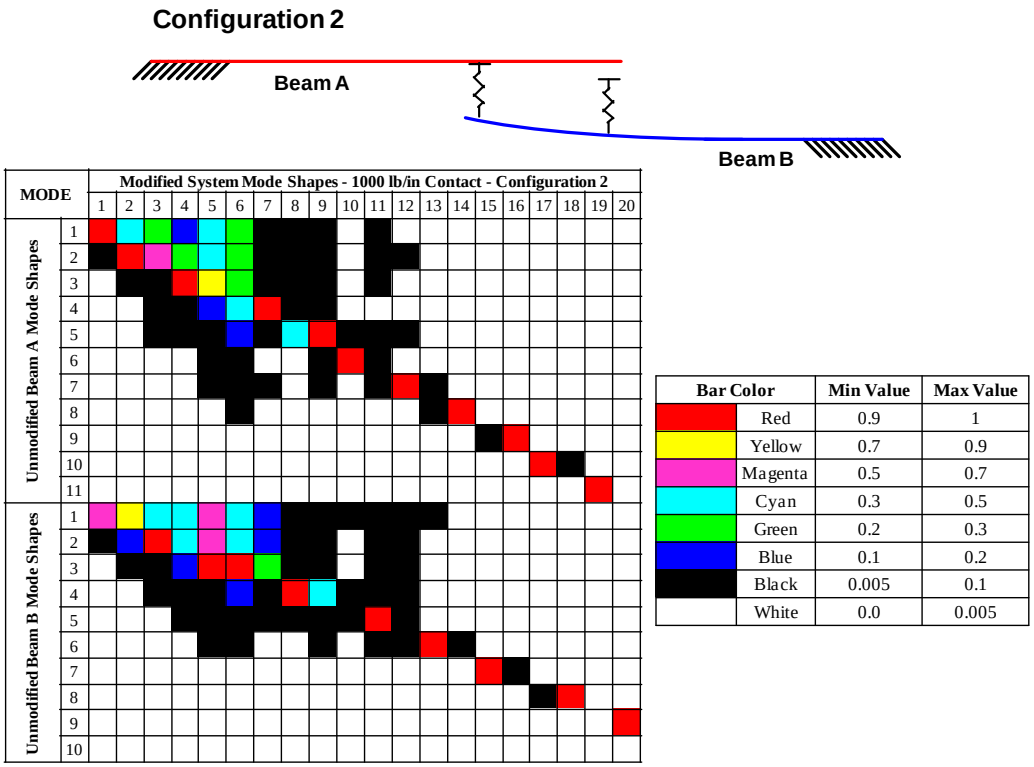

Bar Color		Min Value	Max Value
	Red	0.9	1
	Yellow	0.7	0.9
	Magenta	0.5	0.7
	Cyan	0.3	0.5
	Green	0.2	0.3
	Blue	0.1	0.2
	Black	0.005	0.1
	White	0.0	0.005

Figure 10. Two Beams with Hard Contacts Config. 2 Mode Contribution Matrix

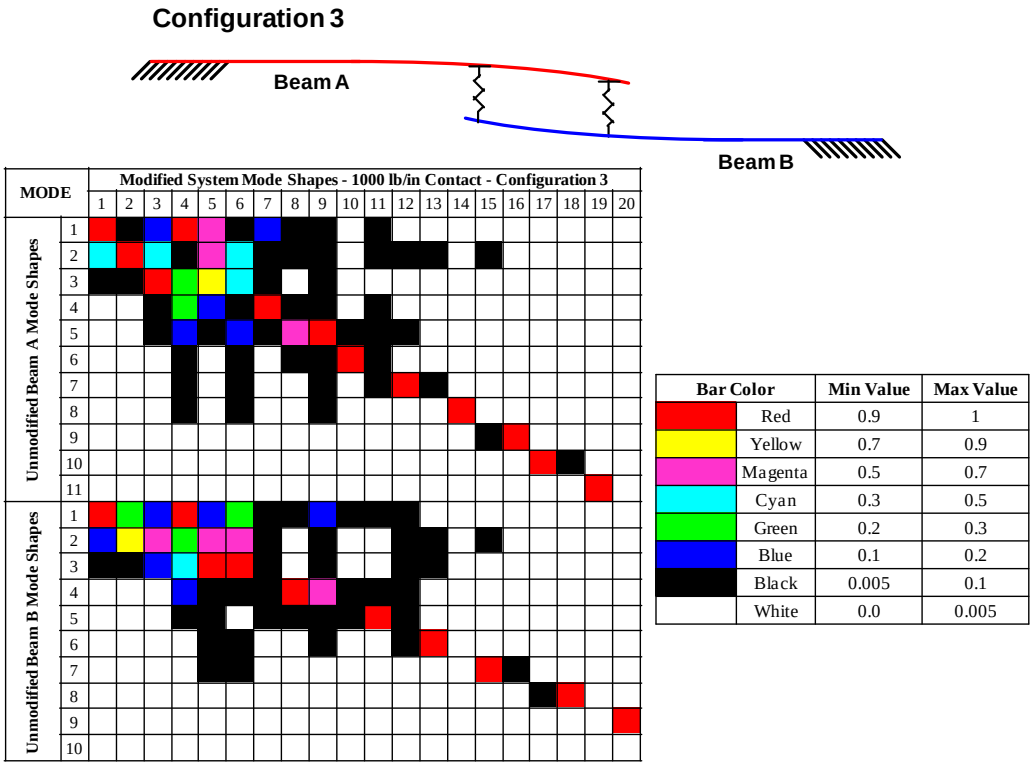

Bar Color		Min Value	Max Value
	Red	0.9	1
	Yellow	0.7	0.9
	Magenta	0.5	0.7
	Cyan	0.3	0.5
	Green	0.2	0.3
	Blue	0.1	0.2
	Black	0.005	0.1
	White	0.0	0.005

Figure 11. Two Beams with Hard Contacts Config. 3 Mode Contribution Matrix

Although each mode contribution matrix is different, the left hand side of the matrices shows that all potential system modes are formed from the original modal database, although the contribution from each mode changes depending on the configuration. As a result, the transformation matrix that contains the original component mode shapes has the necessary information to expand any of the possible states of the system. In order to expand time response data, however, the transformation matrix used must contain an appropriate selection of modes that are needed for accurately forming the potential system modes. This was demonstrated by Thibault [16], who showed that an imperfect FEM could be used to accurately expand test data provided that a sufficient selection of modes were included in the transformation matrix developed from the FEM; details of the VIKING technique are beyond the scope of this paper and is discussed in greater detail in [16].

There are two key statements in the theory listed above that allow the work listed in this paper to be performed.

1. The time response solution can be expanded out to full space using the transformation matrix developed from the mode shapes. This has been demonstrated by Chipman [1] and Pingle [2] for linear cases.
2. An imperfect transformation matrix can be used to expand test data correctly provided sufficient modes are included. This was demonstrated by Thibault [16] who accurately expanded mode shapes with an imperfect transformation matrix.

As a result of these two statements, the following statement can be developed. An imperfect transformation matrix (one obtained from linear reduction of components) can be used to expand a nonlinear time solution (one formed from a different set of modes at a given time) provided sufficient modes are included. This will be demonstrated with an analytical and experimental case study in the following section.

MODEL DESCRIPTION AND CASES STUDIED

Model Description

Due to the complexity of the nonlinearities introduced into actual structural systems, a representative structure was fabricated to demonstrate the proposed technique. The laboratory structure is comprised of two cantilevered aluminum beams that are mounted to a common frame and base plate, as shown in Figure 12. Beam A is shown in red and Beam B is shown in blue to distinguish the two components apart from one another. This structure was designed to be a simplified representation of a typical structural system that contains various contact and component interconnection features, such that the forced nonlinear response of the system would have similarities to real-world structures of interest.

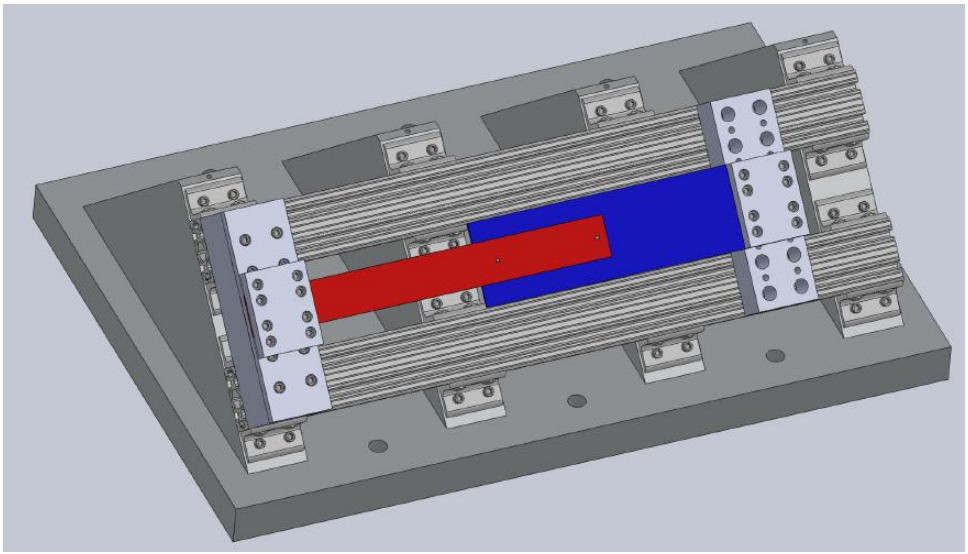

Figure 12. Laboratory Structure Representation of Contact Nonlinearities

Two planar beam element models were generated using MAT_SAP [17], which is a finite element modeling (FEM) program developed for MATLAB [18]. Each beam model is clamped for 3 inches of their length using translational and

rotational springs to replicate the cantilevered boundary condition that is applied in the actual test fixture shown in Figure 12. Table 1 lists the dimensions, material properties, and modeling characteristics of the beam component models.

Table 1. Beam Model Characteristics

Property	**Beam A**	**Beam B**
Length (in)	18	16
Width (in)	2	4
Thickness (in)	0.123	0.123
# of Elements	72	64
# of Nodes	73	65
# of DOF	146	130
Node Spacing (in)	0.25	0.25
Material	Aluminum	Aluminum
Density (lb/in^3)	0.098	0.098
Young's Modulus (Msi)	10	10

An eigensolution was then computed for the component models. Table 2 lists the natural frequencies for the first 10 bending modes of each beam component model, where bending about the weaker axis is implied. Torsional modes are not included because the input excitation and nonlinear contact locations are assumed to occur along the centerline of the beams.

Table 2. Natural Frequencies of Beam Models

Mode #	**Frequency (Hz)**	
	Beam A	**Beam B**
1	12.915	22.625
2	84.119	141.561
3	252.339	396.604
4	519.587	776.916
5	806.163	1284.714
6	1256.551	1918.277
7	1682.965	2678.333
8	2201.360	3563.885
9	2755.524	4572.697
10	3510.011	5707.037

The cantilevered beam component models developed were assembled into common matrix space as a linear system, which was discussed previously and is shown in Figure 13. Note that the FEM nodes for 3 inches of each beam are clamped for the cantilevered boundary condition that was applied using $10E^6$ lb/in translational springs and $10E^6$ lb-in/rad rotational springs. This was performed to simulate the boundary condition that exists on the actual test fixture, where the beams are clamped between a top plate and a base block. Translational and rotational springs were used to allow for fine-tuning of the models in order to account for possible flexibility of the test fixture if this was a concern for the cases where test data is introduced.

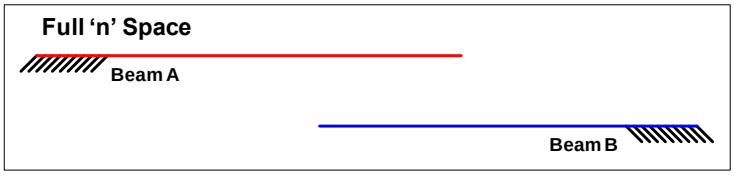

Figure 13. Schematic of Full Space Linear Beam Models

The full space linear component models were then reduced down to 'a' space using SEREP where the ADOF were selected to correspond with transducer locations on the actual tested structure. SEREP reduction was performed for the case where the number of ADOF and modes retained in the reduced order models are equal. Therefore, the selection of ADOF does not affect the reduced model characteristics. In addition, the DOF at potential contact locations were retained in the reduction process in order to formulate system models for possible contact configurations. The full space and reduced space component models are shown in Figure 14, where the red points indicate the ADOF retained in the reduced order models and the black arrow denotes the force pulse input location, which is at DOF 105 of Beam A. The ADOF and modes retained in the reduced component models are listed in Table 3. Note that only translational DOF were retained in the reduced component models.

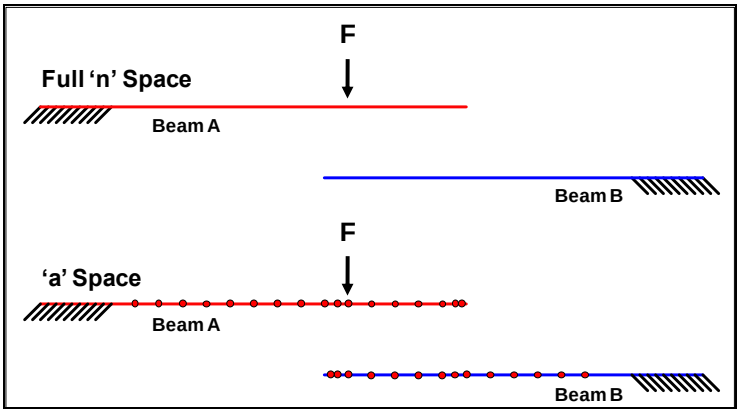

Figure 14. Full Space and Reduced Models with Force Pulse Input Location

Table 3. ADOF and Modes Retained in Reduced Beam Models

Reduced Model	# of DOF	Retained Modes	Retained DOF
Beam A 'a' Space	17	1-17	33,41,49,57,65,73,81,89,97,101, 105,113,121,129,137,141,143
Beam B 'a' Space	14	1-14	149,151,155,163,171,179,187, 191,195,203,211,219,227,235

An analytical force pulse was designed to be frequency band-limited, exciting modes up to 1000 Hz while minimally exciting higher order modes. The force pulse was applied at DOF 105 of Beam A for all analytical cases studied. The force pulse input DOF was selected to avoid being located at the node of a mode, where minimal response of a particular mode could result.

When computing the system response to the input force pulse using the Newmark direct integration method [19], the initial conditions defined at time t = 0 were zero initial displacement and zero initial velocity. The time step (Δt) used was 0.0001 seconds. An additional parameter that was used in the direct integration process was damping. For the analytical models developed in this work, the modal damping ζ, for all component modes as well as for all system modes was assumed to be 1 % of critical damping.

Analytical Case Study

Although many cases were studied [3], the case described here consists of Beam A coming into contact with Beam B in three different configurations at two possible contact locations once a specified gap distance is closed between Beams A and B, which is 0.05 inches for this case, as was previously shown in Figure 4. Each system is a potential configuration of the two components depending on the relative displacements of the two beams where no contact is also a possible configuration.

The spring element used at the contact locations was a 1000 lb/in translational spring and can be considered to be a relatively hard contact for the system studied in this work. The spring stiffness is applied to the full space physical model for each system configuration and an eigensolution is computed using the modified system mass and stiffness matrices. The contact for configuration 1 occurs between DOF 141 of Beam A and DOF 191 of Beam B. The contact for configuration 2 occurs between DOF 101 of Beam A and DOF 151 of Beam B. The contact for configuration 3 occurs when both contacts for configurations 1 and 2 are closed simultaneously. The natural frequencies of the modified system configurations as well as for the unmodified components are listed in Table 4. Figure 9 - Figure 11 shows the mode contribution matrices that are used to identify the unmodified component modes that contribute in the modified system modes for system configurations 1, 2, and 3, respectively. The mode contributions are computed using full space models such that modal truncation is not of concern. The various box colors indicate the amount that each unmodified component mode contributes in a particular modified system mode; the actual contribution ranges for each color are shown.

Table 4. Natural Frequencies for Two Beams with Multiple Hard Contacts – Potential System Configurations 1, 2, and 3

Mode #	**Frequency (Hz)**				
	Modified System - Hard Contacts			**Unmodified Components**	
	Config. 1	**Config. 2**	**Config. 3**	**Beam A**	**Beam B**
1	21.254	15.496	36.217	12.915	22.625
2	67.744	69.517	113.686	84.119	141.561
3	127.044	119.785	228.570	252.339	396.604
4	236.020	234.136	312.678	519.587	776.916
5	338.309	325.850	339.402	806.163	1284.714
6	424.257	467.087	504.557	1256.551	1918.277
7	532.039	527.491	532.406	1682.965	2678.333
8	786.594	786.040	790.327	2201.360	3563.885
9	809.246	828.779	833.736	2755.524	4572.697
10	1256.688	1257.170	1257.216	3510.011	5707.037
11	1294.656	1290.027	1300.104	-	-
12	1682.968	1686.002	1686.011	-	-
13	1918.723	1920.049	1920.475	-	-
14	2201.525	2202.671	2202.844	-	-
15	2683.897	2678.847	2684.381	-	-
16	2755.784	2756.010	2756.282	-	-
17	3510.464	3511.344	3511.794	-	-
18	3564.138	3563.976	3564.234	-	-
19	3948.794	3948.545	3948.795	-	-
20	4575.186	4572.697	4575.187	-	-

For this case, three potential modified system configurations exist, which results in three separate mode contribution matrices. The ‘a’ space reduced model developed for this case retains 17 DOF and modes 1 to 17 of Beam A and 14 DOF and modes 1 to 14 of Beam B. The models developed for this case are shown in Figure 15 for the full- space and reduced ‘a’ space models.

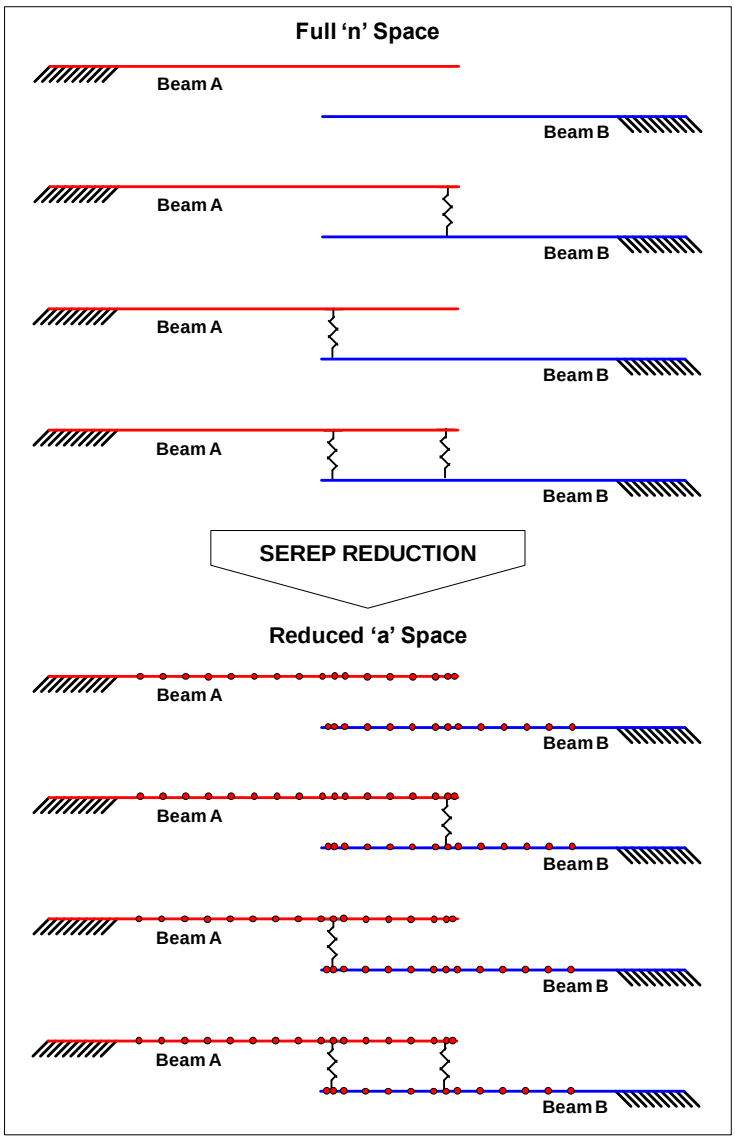

Figure 15. Full Space and Reduced ‘a’ Space Models for Two Beams with Multiple Contacts

To confirm that the 31 DOF ‘a’ space models are sufficient for this case, the system response at DOF 141 is plotted in the time and frequency domain for the reduced model with comparison to the full space solution in Figure 16.

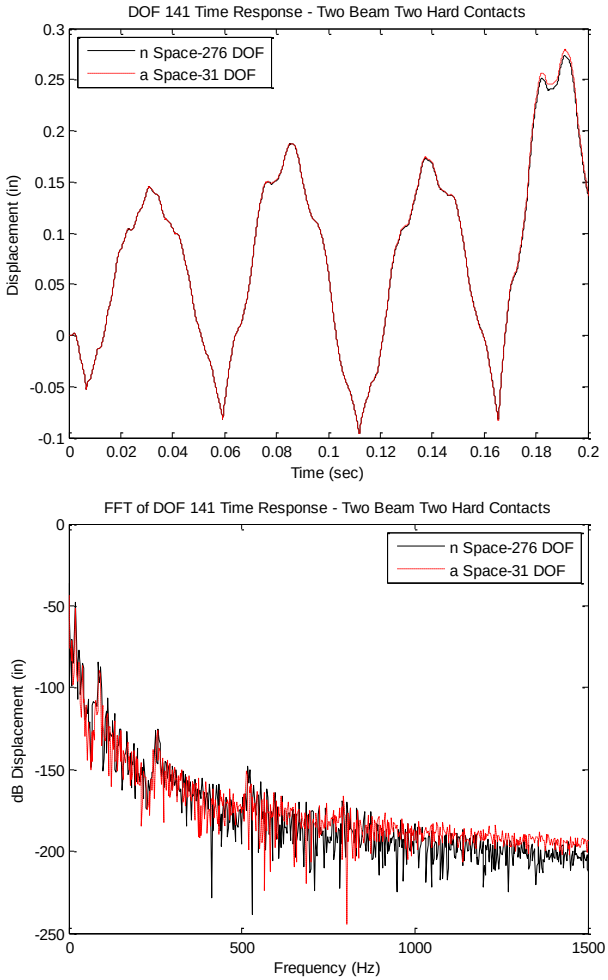

Figure 16. Comparison of 276 DOF 'n' and 31 DOF 'a' Space Models for Two Beams with Multiple Hard Contacts – DOF 141 Time Response (Top) and FFT of Time Response (Bottom)

The results obtained when using the 31 DOF 'a' space model can be observed to correlate very well with the full space solution in Figure 16. Two different time correlation tools MAC and TRAC (Appendix A) are used to quantify the similarity of the reduced model results with the full space solution. Both plots are shown in Figure 17 where the y-axis scale for the MAC and TRAC plots is 0.999-1.0 so that the slight differences between the full space and reduced space solutions could be observed. The solution time for each model is listed with the average MAC and TRAC values in Table 5 to show the significant decrease in computation time and highly accurate results when the reduced models are used.

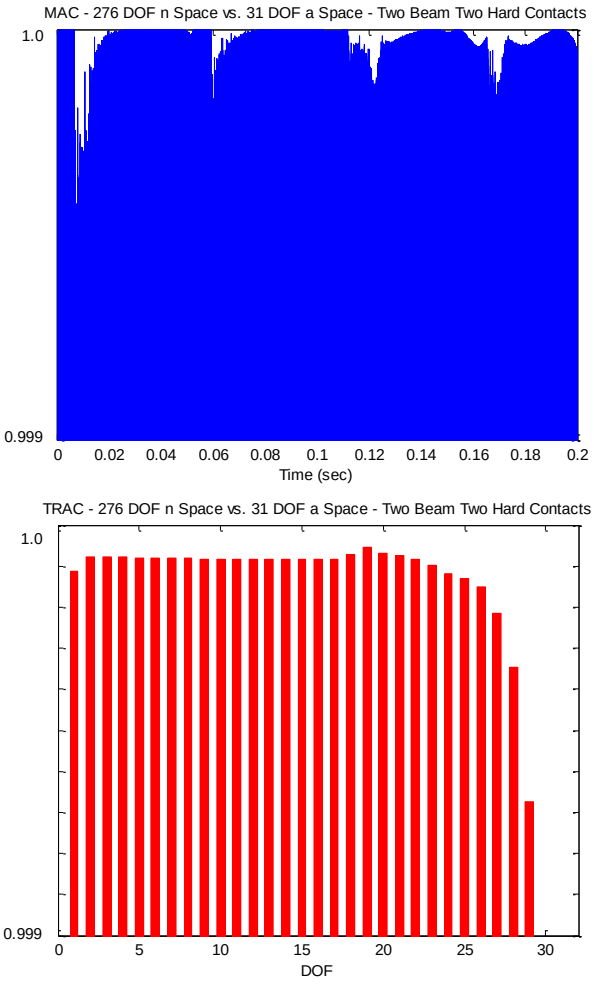

Figure 17. MAC (Top) and TRAC (Bottom) Comparisons Between 276 DOF 'n' and 31 DOF 'a' Space Models for Transient Portion of Time Response (0 to 0.2 Seconds) – Two Beams with Multiple Hard Contacts

The solution obtained using the 'a' space model was then expanded out to 'n' space using the linear transformation matrix developed in Figure 15. Figure 18 shows the MAC and TRAC plots over the first 0.2 seconds (note that the TRAC is now calculated for all 276 DOF). The y-axis scale for the MAC and TRAC plots is 0.9-1.0 so that the slight differences between the full-space and reduced space solutions could be observed. The 276 DOF 'a' space expanded model for the two beam system with multiple hard contacts produces very good results as well.

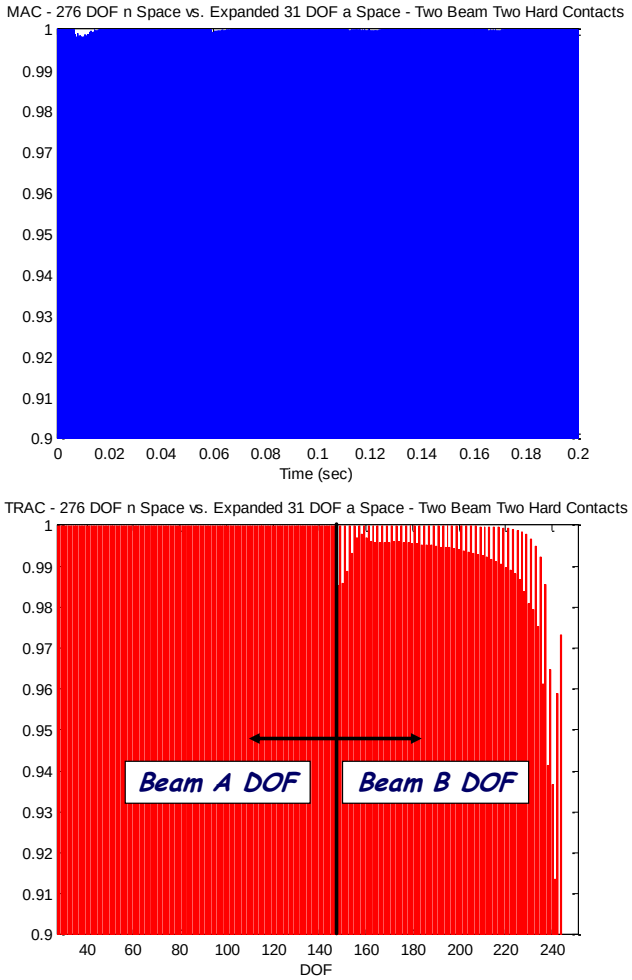

Figure 18. MAC (Top) and TRAC (Bottom) Comparisons Between 276 DOF 'n' and 276 DOF 'a' expanded Space Models for Transient Portion of Time Response (0 to 0.2 Seconds) – Two Beams with Multiple Hard Contacts

The solution times for all models are listed with the average MAC and TRAC values in Table 5 to show the significant decrease in computation time and that highly accurate results are obtained when the reduced models are used. The favorable MAC and TRAC results in Table 5 show that the 31 DOF 'a' space model is sufficient for accurately computing the initial transient portion of the time response for this particular case. In addition, the solution time for the full-space model is 88.5 seconds in contrast to the reduced 'a' space model, which is only 4.9 seconds.

Table 5 also lists the average MAC and TRAC for each solution along with the solution time (the solution time for the expanded 'a' space is the time required to solve the 'a' space model and then expand to 'n' space). Even with the additional calculation due to multiplying the time solution by the expansion matrix, the time required is significantly reduced in comparison to the full 'n' space solution, going from 88.5 seconds to 5.1 seconds. The average MAC and TRAC have negligible improvements because the remaining error is due to truncation which is not improved by expansion of the time responses.

Table 5. Solution Times and Average MAC/TRAC for Two Beams with Multiple Hard Contacts – Transient Portion of Time Response (0 to 0.2 Seconds)

Model	# of DOF	Solution Time (sec)	Average MAC	Average TRAC
'n' Space	276	88.5	0.99996	0.99958
'a' Space	31	4.9		
'n' Space	276	88.5	0.99996	0.99973
'a' Space Expanded	276	5.1		

Table 5 shows that expanding the 'a' space time response to 'n' space yielded an accurate solution while significantly reducing the time required. Rather than solving the full space solution directly, reducing the model and then expanding the solution yielded nearly identical results at a fraction of the time.

The other key point of this case study is that the nonlinear time response was achieved using the modes of the originally uncoupled component beam models. Even though the linear mode shapes used in expanding the time responses were not identical to the mode shapes used when the configuration was in a different linear state, a separate expansion matrix for each nonlinear perturbation was not required. Because a sufficient number of modes have been used to span the space of the analytical model and all perturbed nonlinear variations of the model, the expansion does not distort the data and allows for very accurate expansion for all perturbed configurations of the two beam system. As a result, the highly accurate expanded time solution was obtained very efficiently.

Experimental Case Study

A modal survey was conducted to determine the characteristics of the two beams when mounted to the test fixture. Modal impacts were performed at 15 points on each component, where the impact and transducer locations are shown in a dimensioned schematic in Figure 19 along with the actual tested structure.

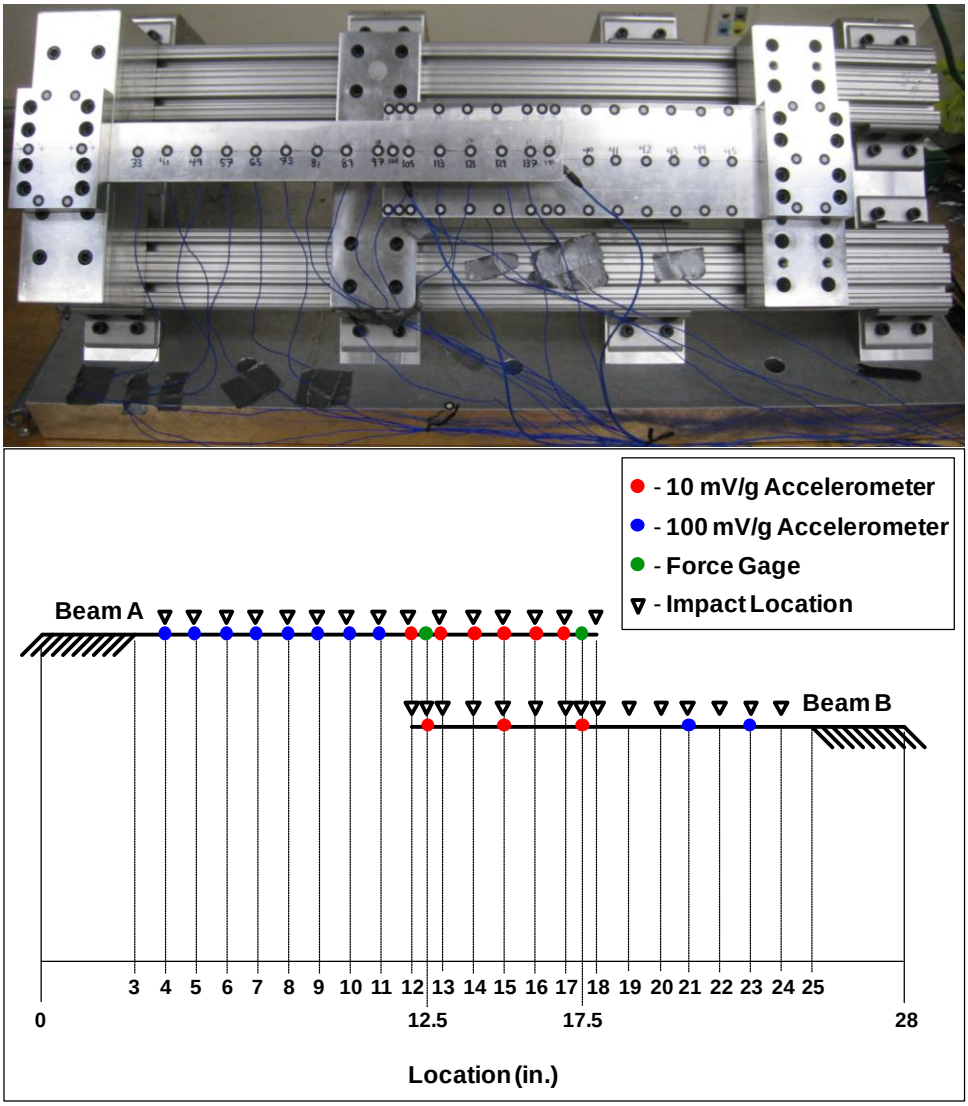

Figure 19. Test Bed with Dimensioned Schematic of Impact and Transducer Locations

To characterize the dynamics of the beams, accelerometer measurements were acquired using LMS Test.Lab 10A [20] and 10 averages were taken for each impact point. Impacts were performed along the centerlines of the beams and only out-of-plane direction motion (normal to beam surfaces) was measured. To extract the desired modal parameters of the tested components, the experimental data was curvefit using PolyMAX [21], which is an advanced modal parameter estimation algorithm implemented within LMS Test.Lab. This provided estimations of the natural frequency, mode shape, and damping characteristics for the system, where the natural frequencies and damping values are listed in Table 6.

Table 6. Natural Frequency and Damping Estimates for Experimental Modal Data

Mode #	Beam A		Beam B	
	Test Frequency (Hz)	Test Damping (% Crit.)	Test Frequency (Hz)	Test Damping (% Crit.)
1	12.850	1.100	23.400	0.440
2	84.970	0.360	144.544	0.100
3	254.270	0.490	405.093	0.090
4	519.510	0.130	797.049	0.060
5	817.240	0.150	1315.013	0.120
6	1234.680	0.200	-	-
7	1637.960	0.360	-	-

The experimentally measured mode shapes consisted of 15 ADOF per component and were expanded out to the full space FEM, which consisted of 146 DOF for Beam A and 130 DOF for Beam B. To perform this expansion, the full space component models were reduced down to retain the 15 tested ADOF for each component. The SEREP reduction scheme was used and therefore, 15 modes for each component were retained in the reduced models in order to formulate a fully ranked transformation matrix. This transformation matrix was then used to expand the test mode shapes out to the full space FEM set of NDOF, which smoothes and completes the measured data. Table 7 lists the correlation results for Beam A, while Table 8 lists the correlation results for Beam B. Both tables show that high correlation between the analytical and test results were obtained with minimal frequency differences (< 2%).

Table 7. Beam A Correlation Results

Mode #	Frequency (Hz)		Frequency (% Diff.)	Original Test		Expanded Test	
	Analytical	Test		MAC	POC	MAC	POC
1	12.915	12.850	-0.502	0.998	0.854	0.990	0.854
2	84.119	84.970	1.001	0.999	0.969	0.999	0.969
3	252.339	254.270	0.759	1.000	1.084	0.999	1.084
4	519.587	519.510	-0.015	0.999	0.949	0.998	0.949
5	806.163	817.240	1.355	0.997	0.957	0.995	0.957
6	1256.551	1234.680	-1.771	0.986	0.913	0.983	0.913
7	1682.965	1637.960	-2.748	0.918	0.882	0.927	0.882

Table 8. Beam B Correlation Results

Mode #	Frequency (Hz)		Frequency (% Diff.)	Original Test		Expanded Test	
	Analytical	Test		MAC	POC	MAC	POC
1	23.029	23.400	1.585	0.993	0.919	0.910	0.919
2	144.456	144.544	0.061	0.994	0.906	0.972	0.906
3	403.340	405.093	0.433	0.991	0.954	0.863	0.954
4	791.173	797.049	0.737	0.980	0.922	0.889	0.922
5	1308.790	1315.013	0.473	0.952	0.910	0.870	0.910

Although multiple cases were studied [3], the case studied here is of a single beam with single contact point. A linear conical spring was mounted to a fixed block to closely resemble a translational DOF spring, as shown in Figure 20. In

addition, the area that the beam impacts the spring is relatively small and is a reasonable approximation of a single DOF, as shown in the red outlined image of Figure 20. The base of the spring is attached to a block that is bolted to the frame of the test bed and can be assumed to be grounded, as shown in the blue outlined image of Figure 20.

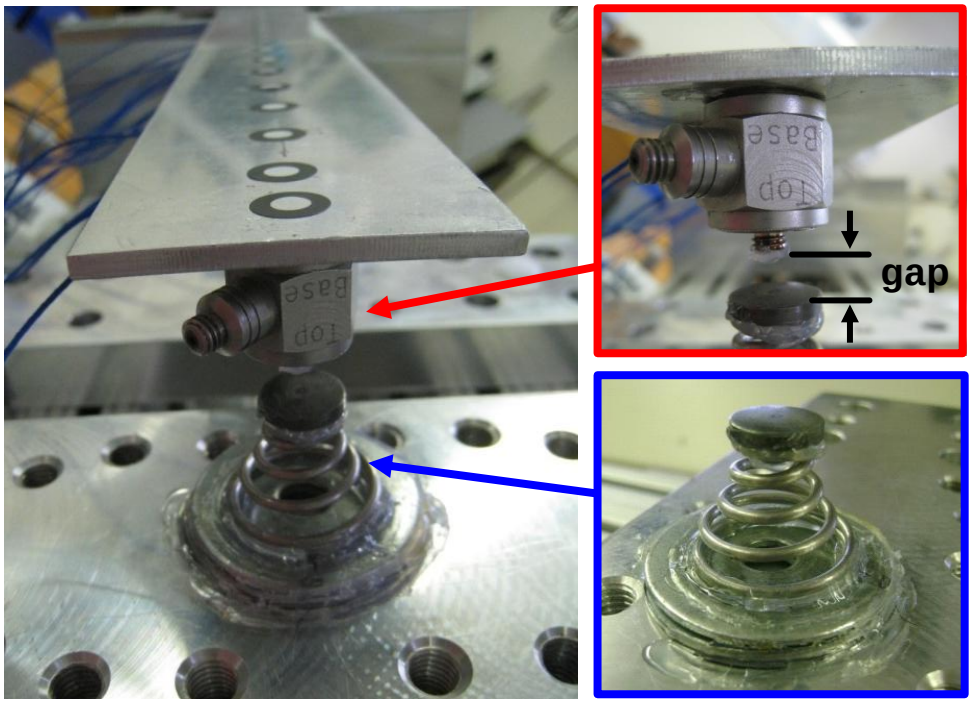

Figure 20. Conical Spring Used for Single Beam with Single Contact Test Case

A force pulse was applied to the single beam using a modal impact hammer. A gap distance of 0.1715 inches was measured between the conical spring and contact thumper attached to the beam, which is shown in the red outlined image of Figure 20. The conical spring was approximated as a single translational DOF stiffness located at DOF 141 and a full space modified system model was developed with the spring stiffness applied. Figure 21 shows the mode contribution matrix where the number of the unmodified component modes needed to form the modified system modes are able to be clearly identified. The various box colors indicate the amount that each unmodified component mode contributes in a particular modified system mode; the actual contribution ranges for each color are shown. The first eight natural frequencies of the modified system as well as for the unmodified component are listed in Table 9.

MODE	Modified System Mode Shapes Conical Spring Contact									
	1	2	3	4	5	6	7	8	9	10
Unmodified Beam A Mode Shapes 1										
2										
3										
4										
5										
6										
7										
8										
9										
10										

Bar Color		Min Value	Max Value
	Red	0.9	1
	Yellow	0.7	0.9
	Magenta	0.5	0.7
	Cyan	0.3	0.5
	Green	0.2	0.3
	Blue	0.1	0.2
	Black	0.005	0.1
	White	0.0	0.005

Figure 21 Mode Contribution Matrix for Single Beam with Conical Spring Contact

Table 9. Natural Frequencies for Single Beam with Conical Spring Contact

Mode #	Frequency (Hz)	
	Unmodified	Conical Spring Contact
1	12.850	41.422
2	84.970	92.352
3	254.270	254.989
4	519.510	519.744
5	817.240	817.297
6	1234.680	1234.686
7	1637.960	1637.960
8	2201.360	2201.365

Accelerometers and PONTOS [22, 23] targets were mounted to the test structure at several locations such that acceleration and displacement time response data could be acquired at collocated points. The system was excited by applying a force pulse into the single beam using a calibrated modal impact hammer. The experimentally measured force pulse was then input to the analytical model to obtain analytical dynamic response predictions for comparison with the test data. The predicted displacement is compared to the measured displacement using PONTOS [23] (high speed digital photogrammetry software) at DOF 81 and DOF 141 over the first 0.2 seconds of the response, as shown in Figure 22.

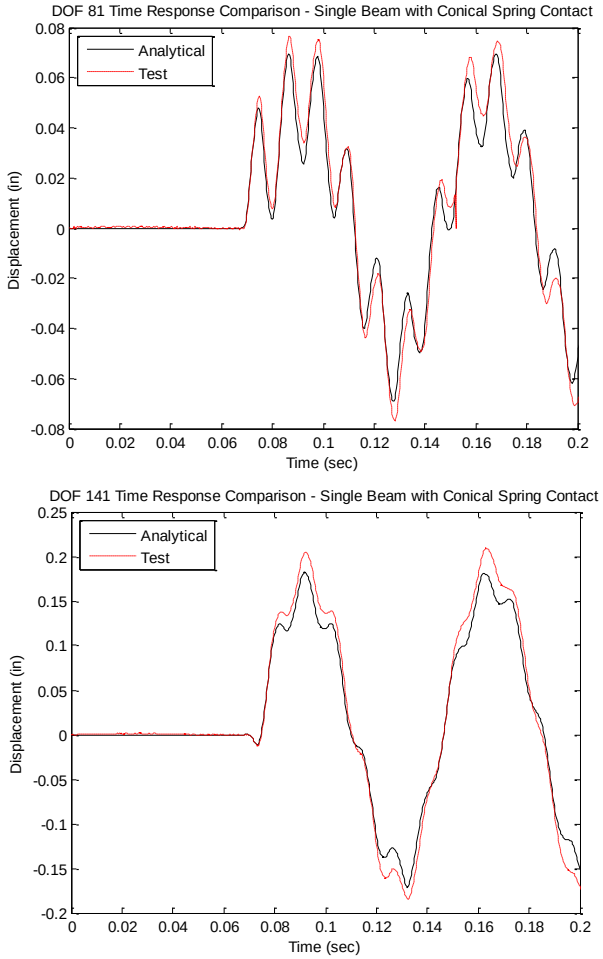

Figure 22. Comparison of Experimental and Analytical Displacements for Single Beam with Conical Spring Contact – DOF 81 (Top) and DOF 141 (Bottom) for Transient Portion of Time Response (0 to 0.2 Seconds)

To quantify the similarity of the reduced analytical model solution with the experimental results, the MAC and TRAC were computed between the reduced analytical model and the experimental time responses, which are shown in Figure 23. Note that the y-axis scale for the MAC and TRAC plots is 0.0-1.0.

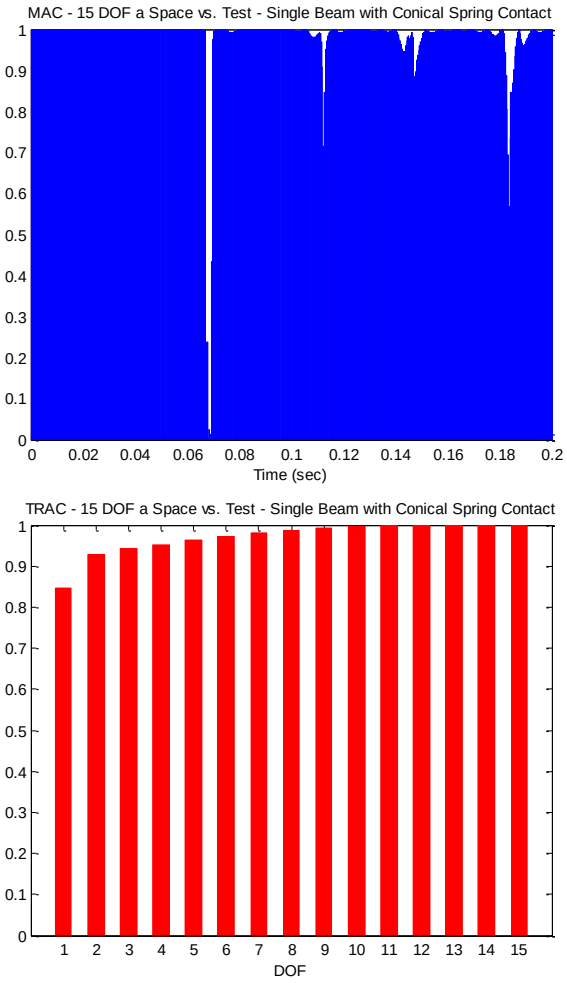

Figure 23. MAC (Top) and TRAC (Bottom) Comparisons Between 15 DOF 'a' Space Model and Test for Transient Portion of Time Response (0 to 0.2 Seconds) – Single Beam with Conical Spring Contact

The results shown in Figure 22 and Figure 23 demonstrate that the analytical model accurately predicts the response when compared to the experimental data for the first 0.2 seconds of the response.

The test results measured at 'a' space were expanded to 'n' space using the linear transformation matrix previously developed and were compared to the 'n' space analytical solution. Figure 24 shows the MAC and TRAC (the TRAC now consists of all 146 DOF). Note that the y-axis scale for the MAC and TRAC plots is 0.0-1.0.

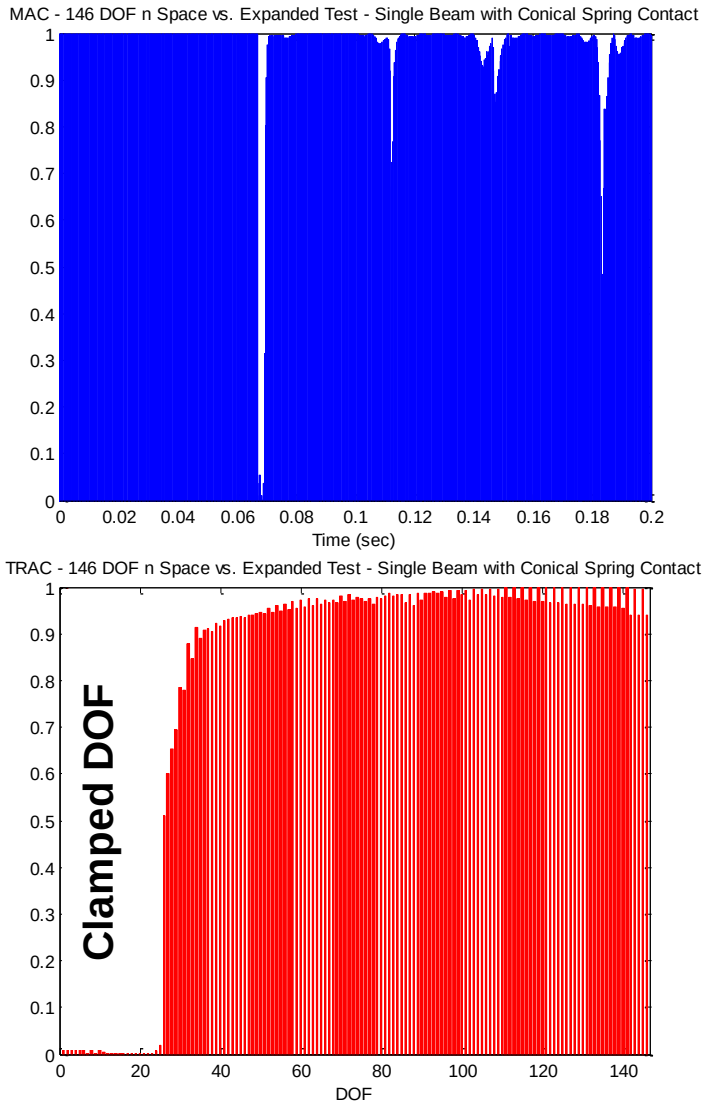

Figure 24. MAC (Top) and TRAC (Bottom) Comparisons Between 146 DOF 'a' Space Expanded Model and Test for Transient Portion of Time Response (0 to 0.2 Seconds) – Single Beam with Conical Spring Contact

As seen in Figure 24, the time response has been expanded and is accurate in comparison to the full field solution. In addition, the time response at DOFs that would be hard to traditionally measure (rotational DOF, DOF with minimal response, or DOF that are not easily accessible for instrumentation) can be obtained. Furthermore, this reduces the need for instrumentation as a subset of measurement points can be used to compute the full field solution instead of attempting to measure the response at every location. Figure 25 displays the correlation between the analytical model and experimental data for DOF 62, a rotational DOF located near the clamped end. Although this would be very difficult to measure traditionally, the expansion shows a high level of correlation.

Table 10 lists the solution times for the full space and reduced space analytical models as well as the average MAC and TRAC comparing the experimental results to the analytical models. As in the previous case, the reduced order model can accurately predict the system response with significant computational savings. Also note that for the experimental case the expanded results improve the MAC and TRAC by smoothing the experimental error. Again, the additional time required to expand the time solution is negligible compared to the full field solution.

Table 10. Solution Times and Average MAC/TRAC for Single Beam with Conical Spring Contact – Comparisons Between Analytical Responses and Experimental Data

Model	# of DOF	Solution Time (sec)	Average MAC	Average TRAC
'n' Space	146	312.9	0.97836	0.97006
'a' Space	15	28.3	0.97836	0.97005
'a' Space Expanded	146	28.4	0.98125	0.98049

For this experimental case, good correlation was observed between the experimentally measured and analytically predicted displacement responses for a single beam with conical spring contact. Although small discrepancies were observed between the analytical and test results, the predicted results were considered to provide a sufficient level of correlation to describe the nonlinear behavior of the tested system. This case also further demonstrates the proposed methodology for use in applications where experimental data is available for comparison with the analytical models being used in forced nonlinear response simulations.

Again note that the expansion of this nonlinear response was achieved using the modes of the originally uncoupled linear component beam model. The expansion process did not distort the data of the separate systems or any perturbation of the combined system because a sufficient number of modes have been used to span the space of the system in all of its various configurations. As a result, measurements that are difficult to make experimentally can be accurately obtained by expansion at a fraction of the time required to measure every single location.

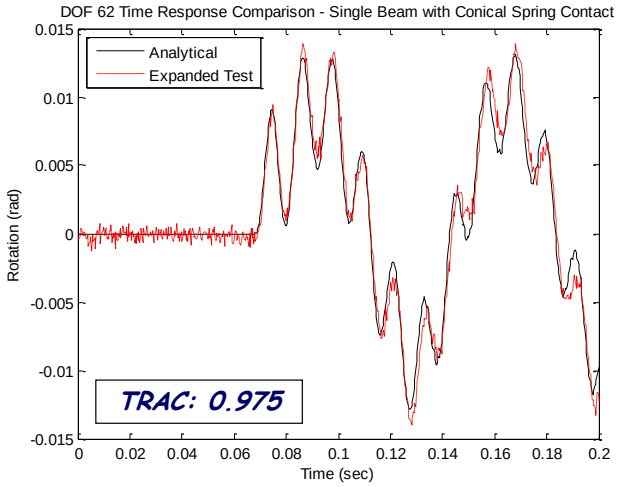

Figure 25. Comparison of Expanded Experimental and Analytical Displacements for Single Beam with Conical Spring Contact – DOF 62 for Transient Portion of Time Response (0 to 0.2 Seconds)

OBSERVATIONS

Reduced order models are computationally advantageous and are useful for many types of applications. Because a full field solution is often desired for visualization purposes, a transformation matrix is often used to expand the limited sets of responses out to the full field solution. This work showed that the same transformation matrix can also be used to expand nonlinear responses, rather than requiring a different matrix for each piecewise linear state of the system. This decreases the computation time required but still gives an accurate solution. This work is especially useful in regards to instrumentation, as it allows a full field solution to be computed from experimental measurements at a limited number of locations.

In addition, the mode contribution matrix was able to be used for identifying the key contributing modes from the original unmodified component models when generating reduced order models. This ensures that the transformation matrix used

for expansion contains all of the modes needed to span the space of the system response, which can be either linear or nonlinear in nature.

CONCLUSION

Previous work demonstrated an efficient approach to nonlinear forced response problems by approximating the nonlinear elements as piecewise linear. The proposed technique in this paper further develops that work by expanding the nonlinear response data using a single transformation matrix formed from the reduction of the individual linear component models. The main advantage of this technique is that only one transformation matrix is needed regardless of the state of the system. In addition, this expansion process is very computationally efficient and allows for reduced model time response solutions to be expanded out to the full space FEM NDOF with negligible increase in solution time.

Two cases were studied: one analytical and one experimental case. The analytical case showed that the expanded data was highly correlated to the full space solution with a noticeable reduction in computation time. The experimental case showed that test data could be expanded to the full set of FEM NDOF to obtain measurements at locations that would be difficult or impossible to measure experimentally (such as rotational DOF or inaccessible DOF). Both cases demonstrated that this expansion technique is a useful extension of the previous work in modeling nonlinear dynamic response using reduced order linear component models.

ACKNOWLEDGEMENTS

Some of the work presented herein was partially funded by Air Force Research Laboratory Award No. FA8651-10-1-0009 "Development of Dynamic Response Modeling Techniques for Linear Modal Components". Any opinions, findings, and conclusions or recommendations expressed in this material are those of the authors and do not necessarily reflect the views of the particular funding agency. The authors are grateful for the support obtained.

NOMENCLATURE

Symbols:

Matrix

$[M]$ Analytical Mass Matrix
$[K]$ Analytical Stiffness Matrix
$[C]$ Physical Damping Matrix
$[U]$ Analytical Modal Matrix
$[\overline{M}]$ Diagonal Modal Mass Matrix
$[\overline{K}]$ Diagonal Modal Stiffness Matrix
$[\overline{C}]$ Diagonal Modal Damping Matrix
$[T]$ Transformation Matrix
$[E]$ Experimental Modal Vectors
$[I]$ Identity Matrix

Vector

$\{e\}$ Experimental Mode Shape
$\{p\}$ Modal Displacement
$\{F\}$ Force
$\{u\}$ Analytical Mode Shape
$\{x\}$ Physical Displacement
$\{\dot{x}\}$ Physical Velocity
$\{\ddot{x}\}$ Physical Acceleration
$\{t\}$ Time Vector

Subscript

1 State 1
2 State 2
12 State 1-2
i Row i
j Column j
n Full Set of Finite Element DOF
a Reduced Set of DOF
d Deleted (Omitted) Set of DOF
U SEREP

Superscript

T Transpose
g Generalized Inverse
k k^{th} Degree of Freedom
-1 Standard Inverse
A Component A
B Component B
AB System AB

Variable

Δt Time Step
ζ Modal Damping

Acronyms:

ADOF Reduced Degrees of Freedom
DOF Degrees of Freedom
ERMT Equivalent Reduced Model Technique
FEM Finite Element Model
MAC Modal Assurance Criterion
MMRT Modal Modification Response Technique
POC Pseudo-Orthogonality Check
SEREP System Equivalent Reduction Expansion Process
TRAC Time Response Assurance Criterion

REFERENCES

1. Chipman, C.C., "Expansion of Real Time Operating Deformations for Improved Visualization," Master's Thesis, University of Massachusetts Lowell, 2009.
2. Pingle, P., Niezrecki, C., Avitabile, P., "Full Field Numerical Stress-Strain from Dynamic Experimental Measured Data," EURODYN 2011, July 2011, Leuven, Belgium.
3. Thibault, L., "Development of Equivalent Reduced Model Technique for Linear Modal Components Interconnected with Nonlinear Connection Elements," Master's Thesis, University of Massachusetts Lowell, April 2012
4. Marinone, T., "Efficient Computational Nonlinear Dynamic Analysis Using Modal Modification Response Technique," Master's Thesis, University of Massachusetts Lowell, 2012.
5. Guyan, R.J., "Reduction of Stiffness and Mass Matrices," American Institute of Aeronautics and Astronautics Journal, Vol. 3, No. 2, February 1965, p. 380.
6. Kidder, R.L., "Reduction of Structure Frequency Equations," American Institute of Aeronautics and Astronautics Journal, Vol. 11, No. 6, June 1973, p.892.
7. O'Callahan, J.C., "A Procedure for an Improved Reduced System (IRS) Model," Proceedings of the Seventh International Modal Analysis Conference, Las Vegas, Nevada, February 1989.
8. O'Callahan, J.C., Avitabile, P., Riemer, R., "System Equivalent Reduction Expansion Process," Proceedings of the Seventh International Modal Analysis Conference, Las Vegas, Nevada, February 1989.
9. Kammer, D.C., "A Hybrid Approach to Test Analysis Model Development for Large Space Structures," submitted for publication in Journal of Spacecraft and Rockets, November 1989.
10. Marinone, T., Butland, A., Avitabile, P., "A Reduced Model Approximation Approach Using Model Updating Methodologies," Proceedings of the Thirtieth International Modal Analysis Conference, Jacksonville, Florida, February 2012.
11. Thibault, L., Avitabile, P., Foley, J., Wolfson, J., "Equivalent Reduced Model Technique Development for Nonlinear System Dynamic Response," Proceedings of the Thirtieth International Modal Analysis Conference, Jacksonville, Florida, February 2012.
12. Avitabile, P., "Twenty Years of Structural Dynamic Modification – A Review," Sound and Vibration Magazine, Vol. 37, No. 1, January 2003, pp. 14-27.
13. Pingle, P., Avitabile, P., "Prediction of Full Field Dynamic Stress/Strain from Limited Sets of Measured Data," Proceedings of the Twenty-Eighth International Modal Analysis Conference, Jacksonville, Florida, February 2010.
14. Pingle, P., Avitabile, P., "Full Field Dynamic Stress/Strain from Limited Sets of Measured Data," Proceedings of the Twenty-Ninth International Modal Analysis Conference, Jacksonville, Florida, February 2011.
15. Pingle, P., "Prediction of Full Field Dynamic Stress/Strain from Limited Sets of Measured Displacement Data," Doctoral Dissertation, University of Massachusetts Lowell, 2010.
16. Thibault, L., Butland, A., Avitabile, P., "Variability Improvement of Key Inaccurate Node Groups – VIKING," Proceedings of the Thirtieth International Modal Analysis Conference, Jacksonville, Florida, February 2012.
17. MAT_SAP/MATRIX, A general linear algebra operation program for matrix analysis, Dr. John O'Callahan, University of Massachusetts Lowell, 1986.
18. MATLAB R2010a, The MathWorks Inc., Natick, M.A.
19. Newmark, N.M., "A Method of Computation for Structural Dynamics," Journal of the Engineering Mechanics Division, American Society of Civil Engineers, Vol. 85, No. 3, July 1959, pp. 67-94.
20. LMS Test.Lab 10A, LMS International, Leuven, Belgium.
21. PolyMAX, Leuven Measurement Systems, Leuven, Belgium.
22. GOM mbH, Braunschweig, Germany, 2007.
23. PONTOS – GOM mbH, Mittelweg 7-8, 38106 Braunschweig, Germany.
24. Allemang, R.J., Brown, D.L., "A Correlation Coefficient for Modal Vector Analysis," Proceedings of the First International Modal Analysis Conference, Orlando, Florida, February 2007.
25. Van Zandt, T., "Development of Efficient Reduced Models for Multi-Body Dynamics Simulations of Helicopter Wing Missile Configurations," Master's Thesis, University of Massachusetts Lowell, 2006.

APPENDIX A –TIME CORRELATION TOOLS

The correlation tools utilized to compare the results of the expanded real time operating (RTO) [ERTOn] and reference time solution [REFn] are briefly discussed here.

The MAC (Modal Assurance Criteria) [24, 25] as used for this work will identify the correlation of the expanded real time operating displacement solution obtained with the reference solution. The MAC can be computed at each time step t to compare the transient displacement solution with time. The MAC is written as

$$MAC\_RTO = \frac{\left[\{REFn\}^T \{ERTOn\}\right]^2}{\left[\{REFn\}^T \{REFn\}\right]\left[\{ERTOn\}^T \{ERTOn\}\right]} \quad \text{(A-1)}$$

Similar to the MAC, the TRAC (Time Response Assurance Criterion) is a tool used to determine the degree of correlation between two time traces. For the cases presented here, the TRAC is the correlation for one DOF over all time for the expanded time data [ERTOn] compared to the actual measured data [REFn]. The TRAC is written as

$$TRAC\_RTO = \frac{\left[\{REFn(t)\}^T \{ERTOn(t)\}\right]^2}{\left[\{REFn(t)\}^T \{REFn(t)\}\right]\left[\{ERTOn(t)\}^T \{ERTOn(t)\}\right]} \quad \text{(A-2)}$$

The values produced by both the MAC and TRAC will range from 0 to 1; values approaching 1 indicate good correlation.

Also used for comparing the [ERTOn] with reference time solution is an absolute different between the two solutions at each time step. The magnitude of the difference is a measure of how much the [ERTOn] deviates from the reference time solution.

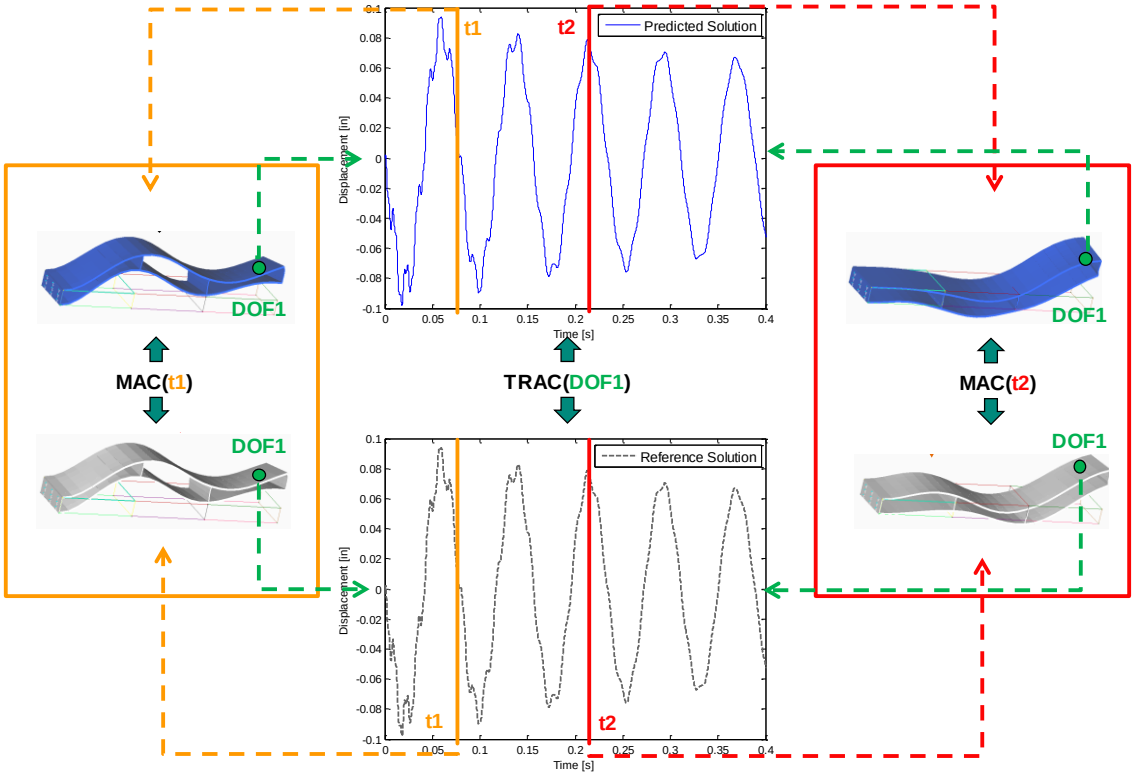

Figure A-1 Schematic showing MAC and TRAC